

## Electronic Supporting Information (ESI)

### Screening Antimonene-Based Single-Atom Catalysts for Nitric Oxide

### Electroreduction to Ammonia by Density Functional Theory Computations

Qiuli Song,<sup>1,#</sup> Zhenghaoyang Zhu<sup>1,#</sup> Yuejie Liu,<sup>2,\*</sup> Peng Wu,<sup>3</sup> Jingxiang Zhao<sup>1</sup>

<sup>1</sup> College of Chemistry and Chemical Engineering, Harbin Normal University, Harbin, 150025, China

<sup>2</sup> Modern Experiment Center, Harbin Normal University, Harbin, 150025, China.

<sup>3</sup> Harbin Taiping Airport Customs, Harbin, 150008, China

\* To whom correspondence should be addressed. Email: liuyuejie@hrbnu.edu.cn (Y. J. Liu)

# Qiuli Song and Zhenghaoyang Zhu contribute equally to this work

## Computational Details

The Gibbs reaction free energy change ( $\Delta G$ ) of each elementary step during the NORR to multicarbon products synthesis was computed by using the computational hydrogen electrode (CHE) model. Based on this model, the  $\Delta G$  value can be obtained by the formula:  $\Delta G = \Delta E + \Delta ZPE - T\Delta S + eU$ , where  $\Delta E$  is the reaction energy of reactant and product species adsorbed on the catalyst directly obtained from DFT computations;  $\Delta ZPE$  and  $\Delta S$  are the changes between the adsorbed species and the gas phase molecules in zero-point energies and entropy at 298.15 K, which can be calculated from the vibrational frequencies, and  $U$  represents the applied potential. Moreover, the NORR catalytic activity was estimated using the limiting potential ( $U_L$ ), computed as  $U_L = -\Delta G_{\max}/e$ , where  $\Delta G_{\max}$  is the free energy change of the most thermodynamically unfavorable elementary step, i.e., the potential-determining step (PDS). The adsorption energy ( $\Delta E_{\text{ads}}$ ) of the NO molecule was computed using the equation:  $\Delta E_{\text{ads}} = E_{*NO} - E^* - E_{NO}$ , where  $E_{*NO}$ ,  $E^*$ , and  $E_{NO}$  are the total electronic energies of the adsorbed NO, catalyst, and the free NO molecule, respectively.

**Table S1.** The distance between the anchored single-atom metals and Sb atoms ( $d_{\text{M-Sb}}$ , Å), the computed binding energies ( $E_{\text{bind}}$ , eV), the difference between the calculated binding energies and the cohesive energies of their respective bulk phases, and the band gap derived from the computed band structures.

M/Sb	$d_{\text{M-Sb}}$	$E_{\text{bind}}$	$E_{\text{bind}} - E_{\text{coh}}$	<i>band gap</i>
V	2.68	-5.77	-0.28	1.10
Cr	2.68	-6.98	-3.20	0.26
Mn	2.67	-4.64	-0.65	0.00
Fe	2.59	-5.60	-0.49	0.45
Co	2.48	-5.14	-0.20	0.00
Ni	2.49	-5.55	-0.39	0.00
Cu	2.56	-4.01	-0.17	0.51
Nb	2.74	-7.04	-7.45	0.00
Mo	2.71	-7.41	-7.03	0.01
Ru	2.56	-7.63	-0.38	0.00
Rh	2.57	-6.96	-0.91	0.15
Pd	2.62	-5.04	-1.34	0.00
Ag	2.73	-3.33	-0.71	0.92
Ta	2.71	-7.29	-7.33	0.22
W	2.69	-6.75	-7.62	0.87
Ir	2.55	-8.09	-0.76	0.00
Pt	2.59	-7.23	-1.70	0.00
Au	2.68	-4.51	-1.43	0.03

**Table S2.** The distance between the anchored single-atom metals and the N ( $d_{\text{N-Metal}}$ , Å), the adsorption strength of NO molecule on these M/Sb catalysts ( $E_{\text{ads}}$ , eV) and the calculated free energies change of  $\Delta G^*_{\text{NO}}$  and  $\Delta G^*_{\text{NHO}}$ .

M/Sb	$d_{\text{N-Metal}}$	$E_{\text{ads}}$	$\Delta G^*_{\text{NO}}$	$\Delta G^*_{\text{NHO}}$
V	1.74	-3.08	-2.19	-0.21
Cr	1.66	-2.44	-1.73	0.62
Mn	1.69	-2.37	-1.65	0.42
Fe	1.68	-2.79	-2.13	0.58
Co	1.65	-2.58	-1.92	0.82
Ni	1.70	-2.05	-1.37	0.61
Cu	1.78	-1.29	-0.59	0.34
Nb	1.85	-4.60	-2.90	-0.59
Mo	1.79	-3.51	-2.79	0.54
Ru	1.77	-3.17	-2.45	0.89
Rh	1.84	-1.91	-1.21	0.50
Pd	1.91	-1.34	-0.66	0.42
Ag	2.09	-0.81	-0.13	0.30
Ta	1.86	-3.72	-3.01	-0.88
W	1.79	-4.16	-3.45	0.52
Ir	1.84	-2.23	-1.54	0.44
Pt	1.91	-1.56	-0.88	0.46
Au	2.05	-0.74	-0.06	0.24

**Table S3.** Computed free energy changes ( $\Delta G$ , eV) for all potential elementary steps involved in the NORR to  $\text{NH}_3$  products on Au/Sb catalysts. Favorable steps are highlighted in red.

Au/Sb	$\Delta G$
$* + \text{NO} \rightarrow *\text{NO}$	-0.06
$*\text{NO} + \text{H}^+ + \text{e}^- \rightarrow *\text{NHO}$	0.24
$*\text{NO} + \text{H}^+ + \text{e}^- \rightarrow *\text{NOH}$	1.15
$*\text{NHO} + \text{H}^+ + \text{e}^- \rightarrow *\text{NH}_2\text{O}$	-0.32
$*\text{NHO} + \text{H}^+ + \text{e}^- \rightarrow *\text{NHOH}$	0.06
$*\text{NH}_2\text{O} + \text{H}^+ + \text{e}^- \rightarrow *\text{O} + \text{NH}_3$	-1.69
$*\text{NH}_2\text{O} + \text{H}^+ + \text{e}^- \rightarrow *\text{NH}_2\text{OH}$	-0.38
$*\text{O} + \text{H}^+ + \text{e}^- \rightarrow *\text{OH}$	-0.56
$*\text{OH} + \text{H}^+ + \text{e}^- \rightarrow \text{H}_2\text{O} + *$	-1.02

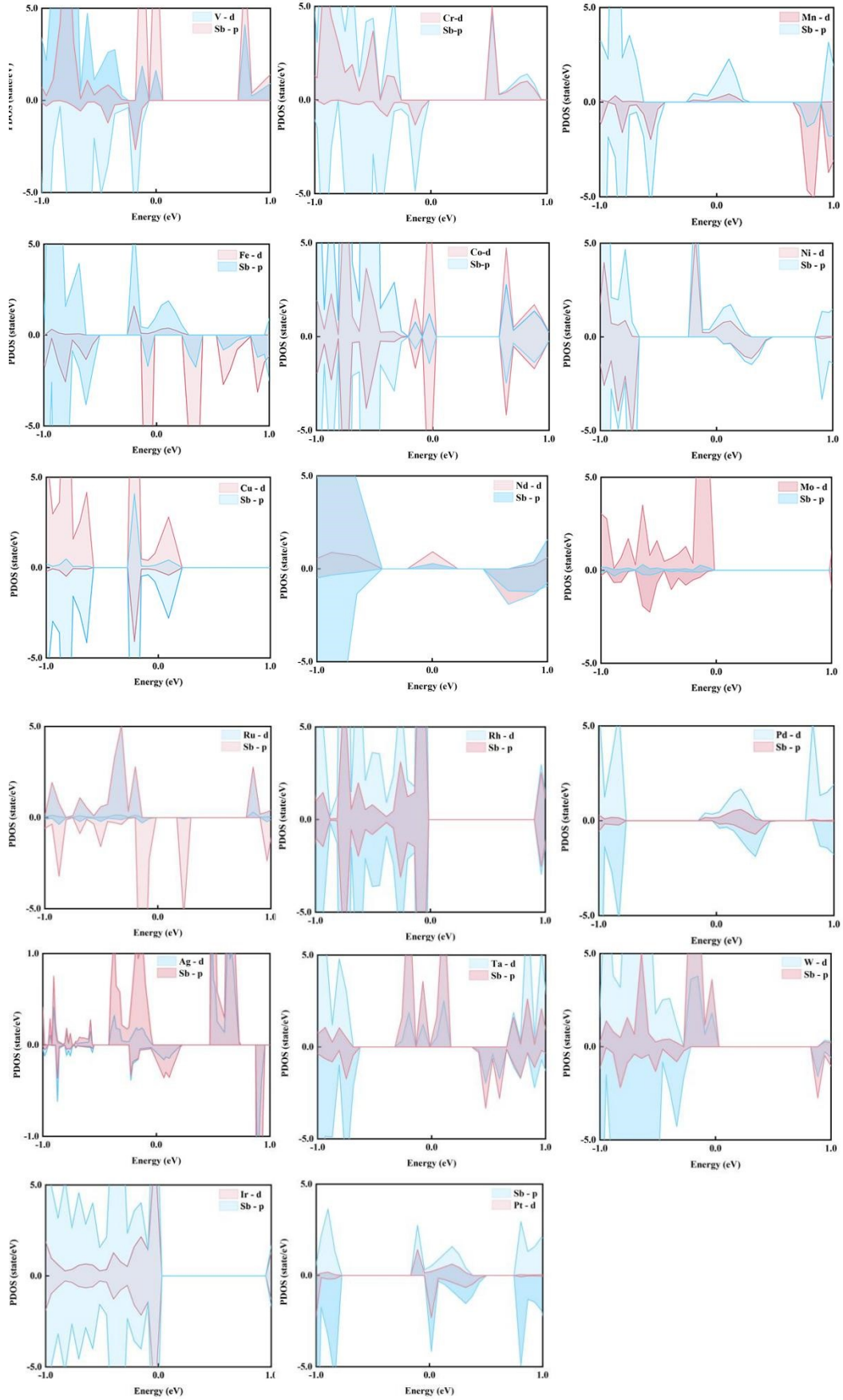


**Fig. S1.** The calculated partial density of states (PDOS) between the metal d-orbitals and Sb p-orbitals in M/Sb catalysts.

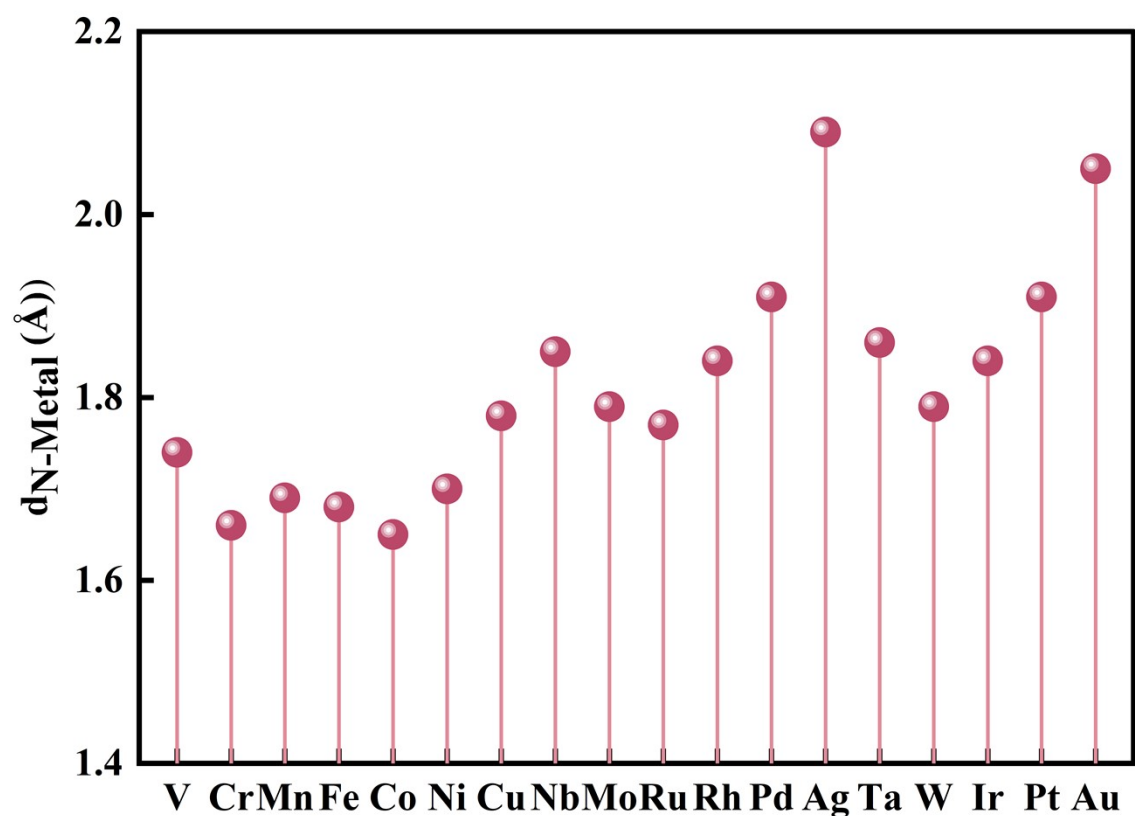


**Fig. S2.** The distance between the anchored single-atom metals and the N ( $d_{N-Metal}$ , Å).

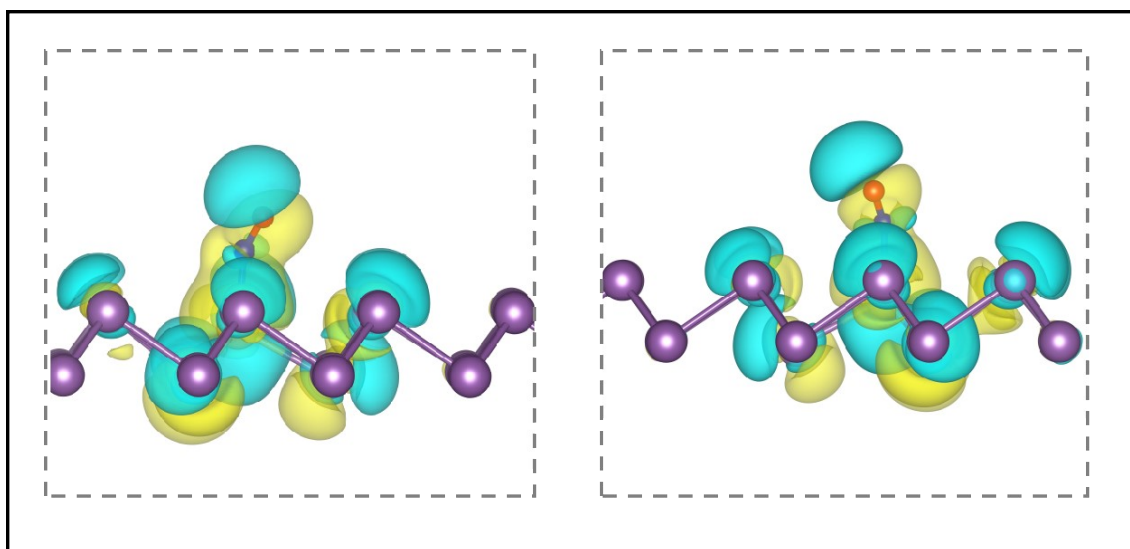


**Fig. S3.** The charge density difference of the NO molecule on the Au/Sb catalyst, where the isosurface value is set to be  $0.005 e \text{ \AA}^{-3}$ , and cyan and yellow bubbles represent positive and negative charges, respectively.

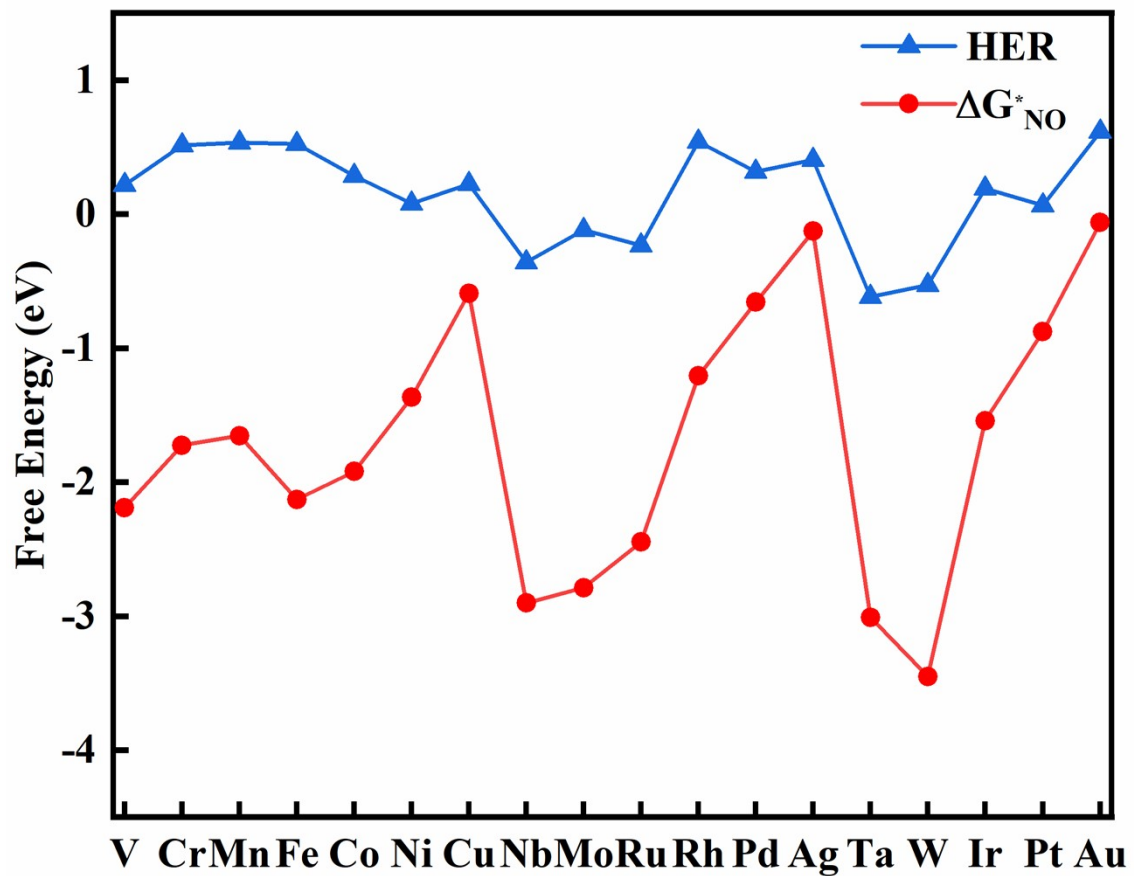
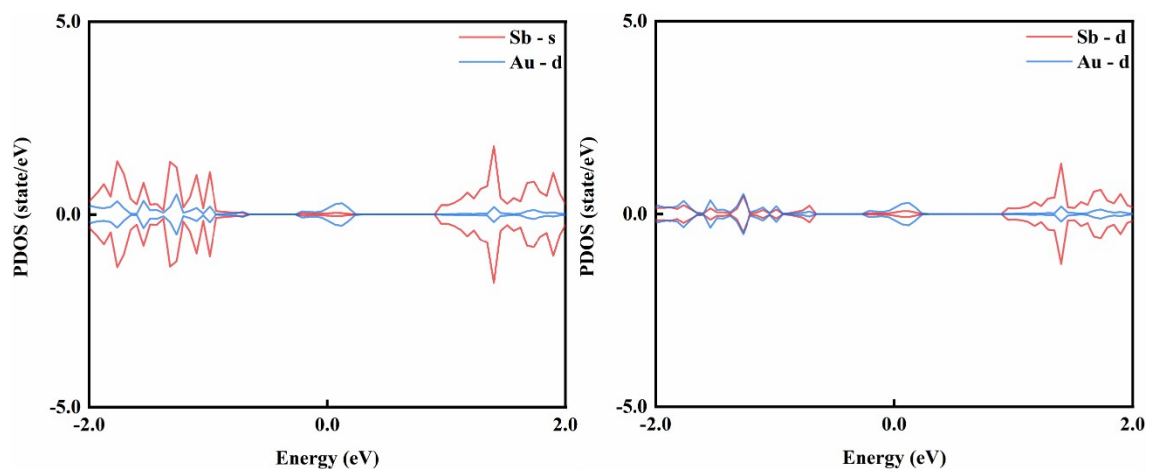
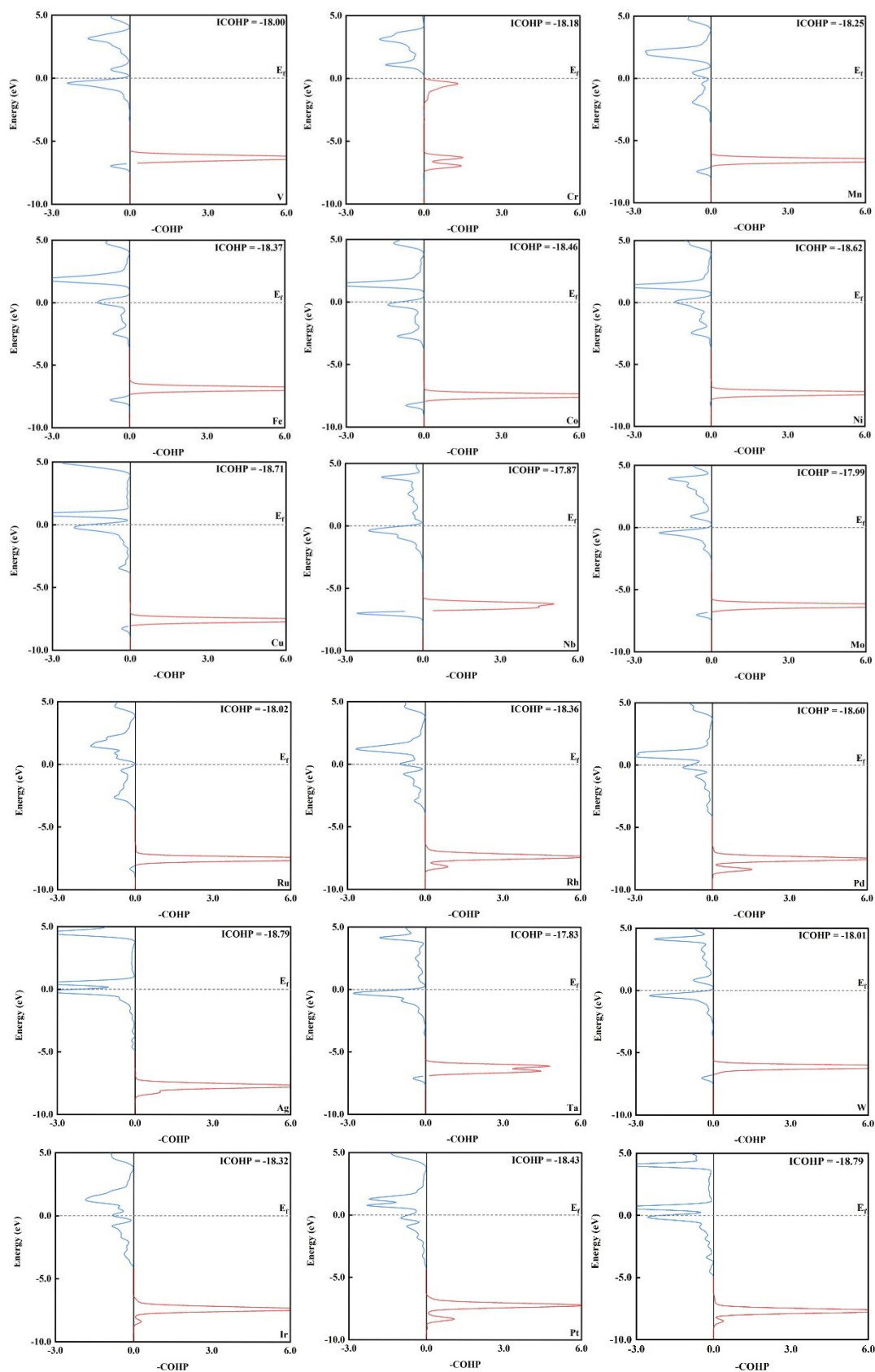


Fig. S4. The calculated Gibbs free energy changes of  $\Delta G^*_{NO}$  and HER.



**Fig. S5.** Electronic partial density of states (PDOS) of Sb-s and Sb-d for the Au/Sb system.



**Fig. S6.** Integrated crystal orbital Hamilton population (ICOHP) of M/Sb.

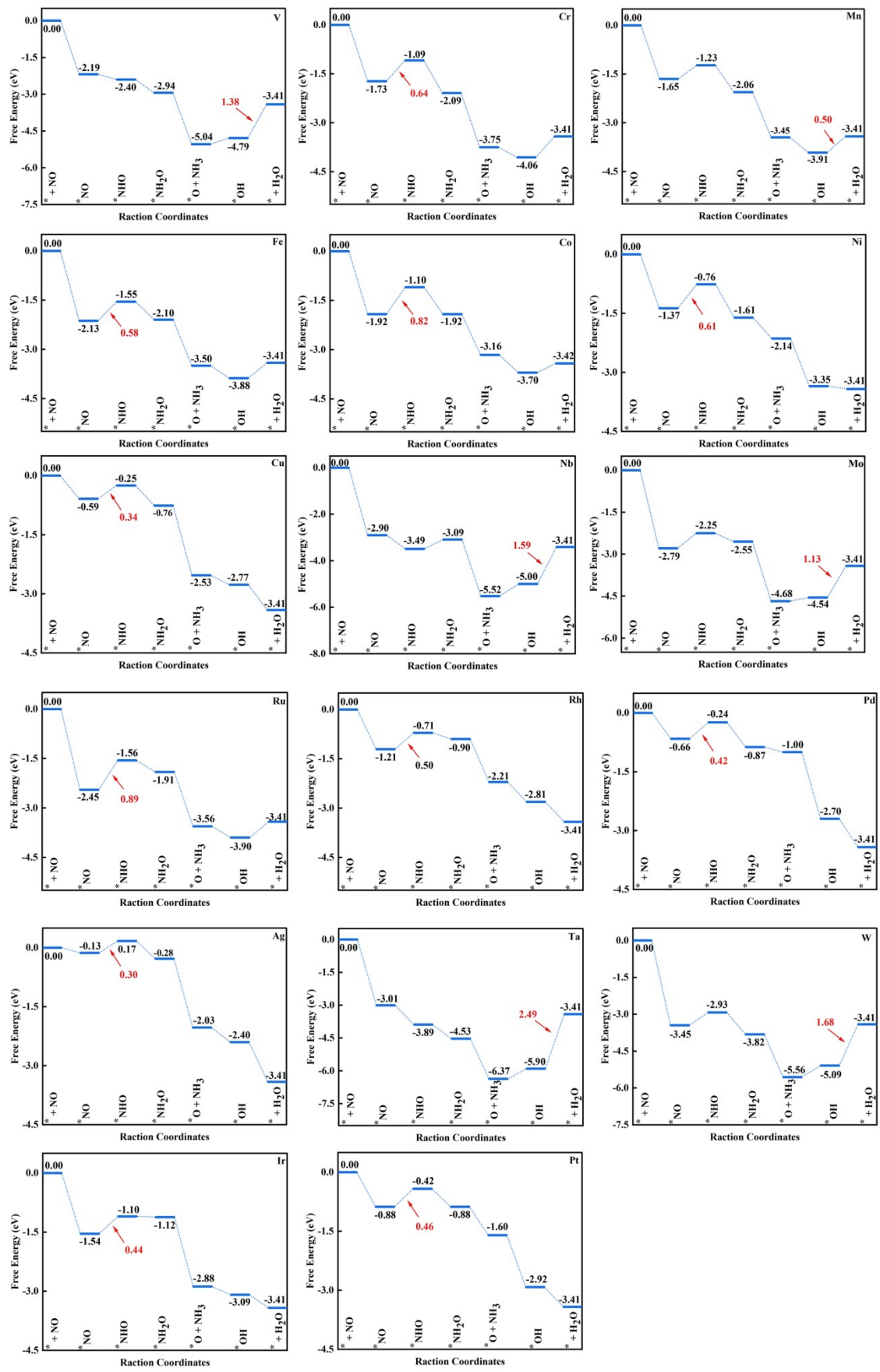


**Fig. S7.** The reaction pathways of NORR to  $\text{NH}_3$  products are considered along possible mechanisms.

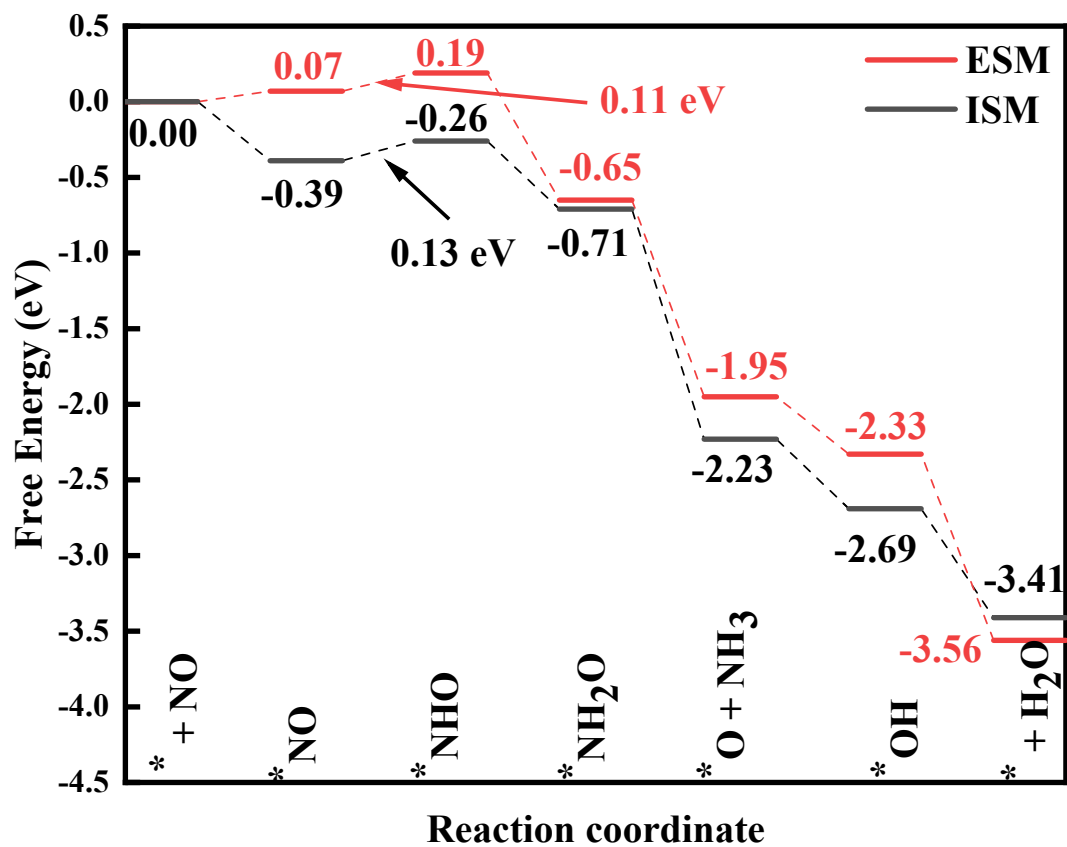


**Fig. S8.** Free energy diagrams for NORR on Au/Sb under implicit solvation (ISM) and explicit solvation (ESM) conditions

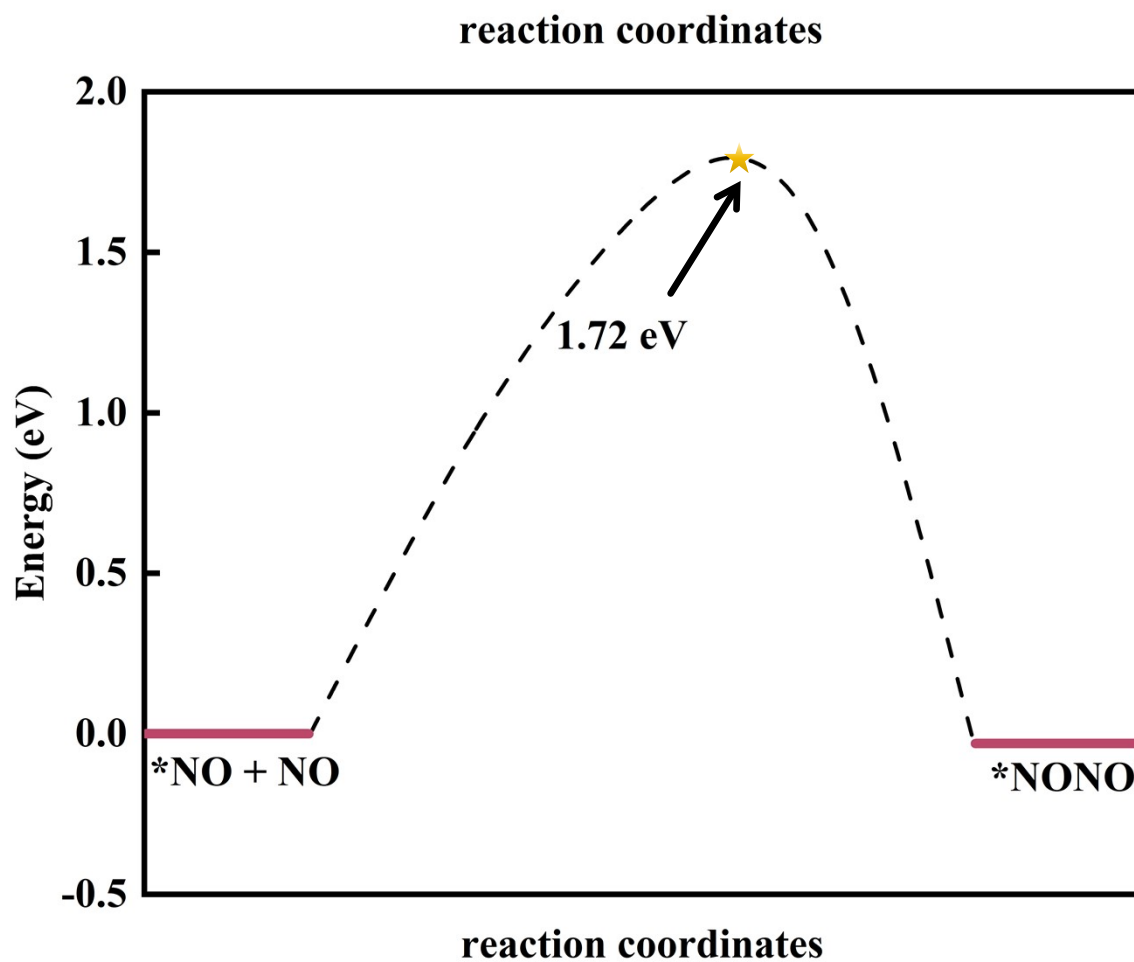
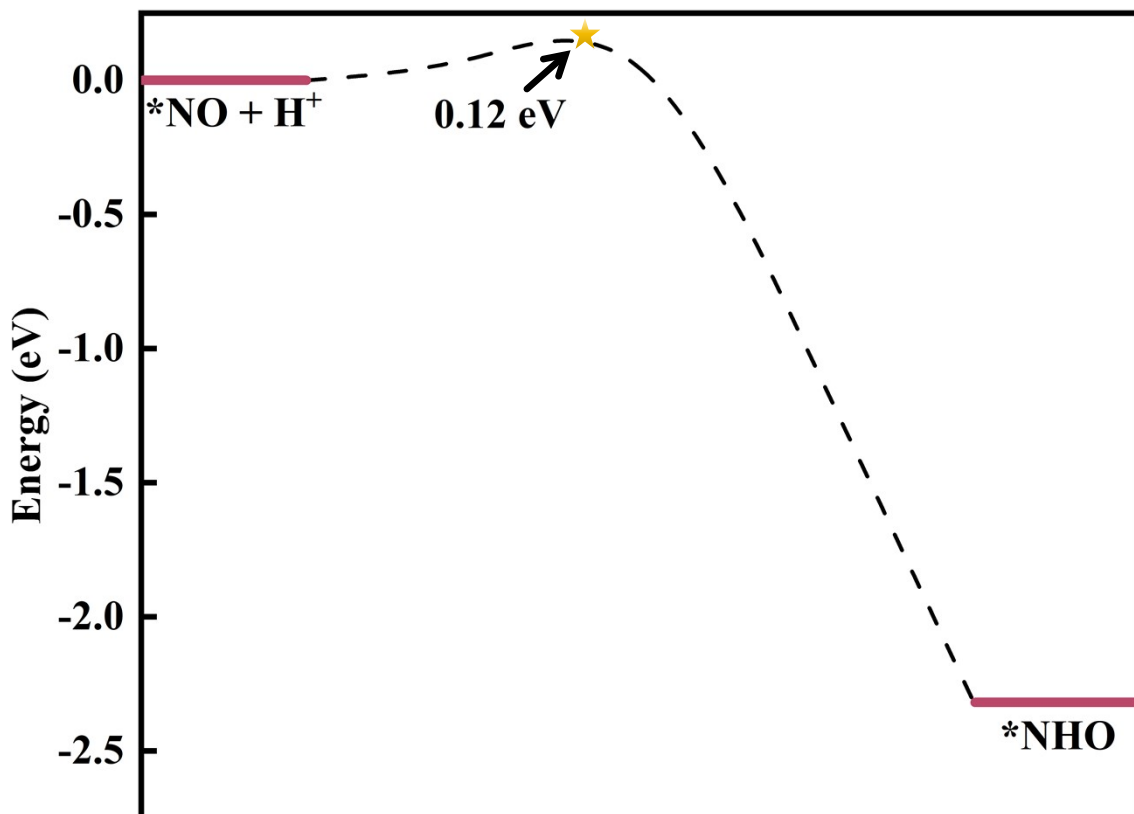


**Fig. S9.** The Kinetic barriers for NO hydrogenation reaction and  $^*N_2O_2$  formation on Au/Sb surfaces.

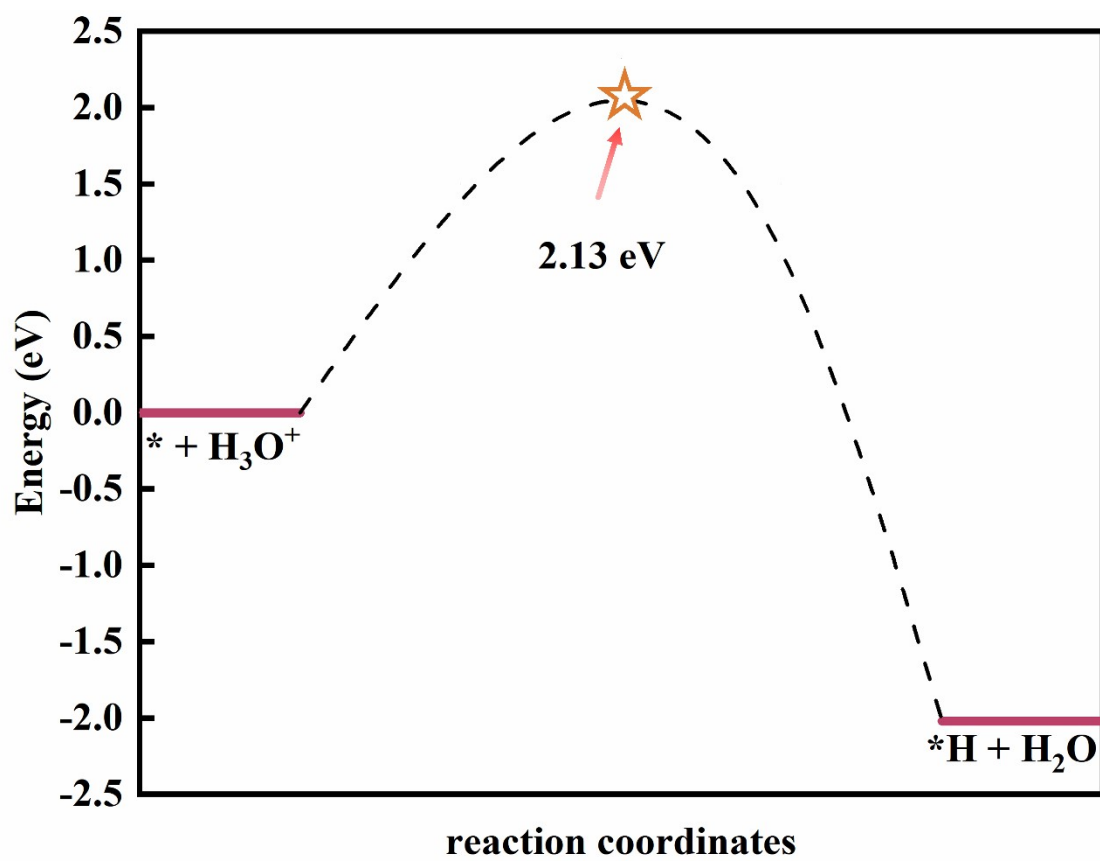


**Fig. S10.** Kinetic energy barrier for \*H adsorption supplied by H<sub>3</sub>O<sup>+</sup> on the Au/Sb surface.